

A&A manuscript no.

(will be inserted by hand later)

Your thesaurus codes are:

(08.06.2 stars:formation 08.16.5 stars:pre-main sequence 09.08.2 Herbig-Haro objects 09.10.1 ISM: jets and outflows 13.09.6 Infrared:stars 02.01.2 Accretion, accretion disks )

ASTRONOMY  
AND  
ASTROPHYSICS

# Shocked Molecular Hydrogen from RNO 91

M. S. Nanda Kumar<sup>1</sup>, B. G. Anandarao<sup>1</sup> & C.J. Davis<sup>2</sup>

<sup>1</sup> Physical Research Laboratory, Navrangpura, Ahmedabad, India - 380009  
e-mail:nanda@prl.ernet.in,anand@prl.ernet.in

<sup>2</sup> Joint Astronomy Center, 660 N. A'ohōkū Place, University Park,Hilo, HI 96720, USA  
e-mail:cdavis@jach.hawaii.edu

6october1998

**Abstract.** We report the detection of the H<sub>2</sub>  $v=1-0$  S(1) line at 2.122 $\mu$ m, from RNO 91 in the L43 dark cloud, which is known to be a T Tauri star surrounded by a 1700AU disk structure (containing ices) and a weak outflow. The non-detection of the H<sub>2</sub>  $v=2-1$  S(1) line at 2.247 $\mu$ m suggests shock excitation rather than fluorescence. The emission is extended spatially up to 9'' in the north-south direction. The line intensity peak (FWHM  $\sim$  3'') corresponds to the star RNO 91 which is embedded in a cocoon of gas and dust. The observed H<sub>2</sub> emission from this cocoon may be attributed to embedded Herbig-Haro like knots. The H<sub>2</sub> line flux in the central 2''  $\times$  3'' is estimated to be  $7 \times 10^{-14}$  ergs sec<sup>-1</sup>cm<sup>-2</sup>, which indicates a mass flow rate of  $4 \times 10^{-8}$  M<sub>⊙</sub> yr<sup>-1</sup>. Furthermore, narrow band image taken through H<sub>2</sub> 1-0 S(1) filter is presented, which reveal a tilted disk and bipolar outflow structure that agrees with earlier observations and models. We show that this disk/outflow system is a unique case.

**Key words:** stars: formation - infrared: spectrum - outflows: HH knots - stars: pre-main-sequence

## 1. Introduction

The near-IR molecular hydrogen emission lines are recognised as being important tools in studies of star formation (Shull & Beckwith 1989). The excitation of these lines involves mainly two competing processes: (i) shock heating and (ii) UV fluorescence (Burton 1992). It is possible, however, to distinguish between these two processes by measuring the ratios of intensities of lines arising from two different vibrational levels (Sternberg & Dalgarno 1989, Hora & Latter 1994). The origin of shocked molecular hydrogen emission from the spatially unresolved region close to the star can originate from outflows or from accretion shocks in a disk, as in the case of Infrared Companions (IRC's) (Herbst et al. 1995, Koresko et al. 1997). RNO 91 ( $\alpha = 16^{\text{h}}34^{\text{m}}29.3^{\text{s}}$ ,  $\delta = -15^{\circ}47'01''$ ) is one of the only two known PMS stars in the L43 dark cloud in

Ophiuchus. It was classified as a M0.5 type T Tauri star by Leverault (1988), based on an optical spectrum that showed strong H $\alpha$  emission. An outflow driven by this star was identified at millimeter wavelengths and shown to have spatially separated red-shifted and blue-shifted lobes (Leverault 1988, Myers et al. 1987, Bence et al. 1998). However, optical images and spectra obtained by Schild et al. (1989) showed that the outflow does not have any emission indicative of shocked material around RNO 91. Optical and infrared photometry (U-band to L-band) was obtained by Myers et al. (1987). Heyer et al. (1990) obtained the JHK photometry and H-band polarimetry of this object which showed a disk type structure for the first time. Weintraub et al. (1994, hereafter, W94) demonstrated by their K-band polarimetric image and 3-5  $\mu$ m spectra that RNO 91 is surrounded by a disk-like structure of radius 1700 AU comprising frozen H<sub>2</sub>O, CO and possibly XCN. They also showed that the polarization center does not coincide with the intensity peak identified as RNO 91. Our speculation that this result indicates an IRC to RNO 91 was quickly laid to rest by the Shift and Add imaging by Aspin et al. (1997) (hereafter A97), which does not show any secondary source within a 3.7'' square region. In this paper we present near-infrared spectra and narrow band images of the object in the K band region. We also report the detection of the H<sub>2</sub>  $v=1-0$  S(1) line at the source and discuss its implications.

## 2. Observations and Data Reduction

Near infrared spectroscopic observations were made on March 25, 1998 at Gurushikhar 1.2 m Infrared Telescope (GIRT), Mt. Abu, India. A Near Infrared Camera / Grating Spectrometer based on a HgCdTe 256  $\times$  256 focal plane array was used to obtain the observations. The grating spectrometer was used in a configuration that yielded a resolving power of  $\lambda/\delta\lambda = 1000$  with a 1''/pixel plate scale. The slit was two pixels wide and oriented along the N-S axis. The atmospheric seeing and image motions were below 2'' during the observations, which was measured from imaging data obtained just before the spectroscopic observations. Data acquisition and reduction were done using

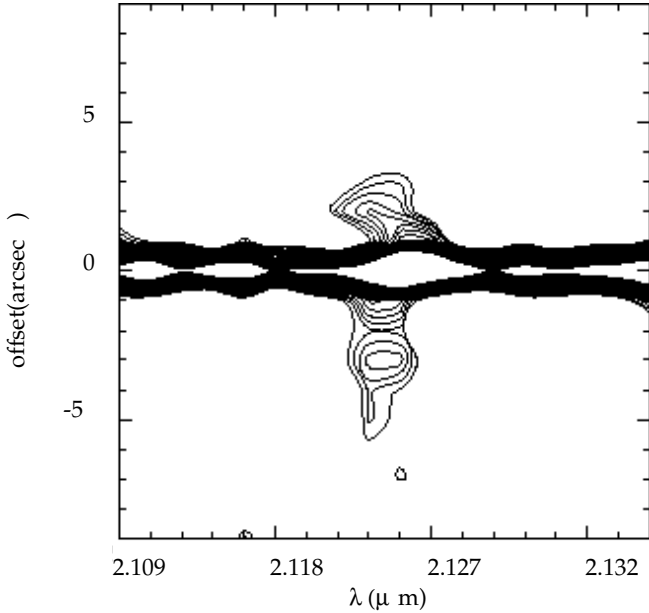


**Fig. 1.** Contours of H<sub>2</sub> 2.122 $\mu$ m line from RNO 91 spectrum showing the extended emission. Notice the different lengths of emission in the N-S from the center that indicates the tilt of the outflow axis. Continuum is *partly subtracted* using an adjacent strip of the same spectrum, which has caused the artifact of width variability.

standard procedures. We used the RNO 91 K band photometric fluxes (0.48 Jy) given by Myers et al. (1987) for flux calibrating the spectrum.

Narrow band ( $\Delta\lambda = 0.02\mu\text{m}$ ) images through H<sub>2</sub> ( $\lambda = 2.122\mu\text{m}$ ), Br $\gamma$  ( $\lambda = 2.165\mu\text{m}$ ) and continuum ( $\lambda = 2.104\mu\text{m}$ ) filters were obtained by the United Kingdom Infrared Telescope (UKIRT) Service Observing Program on September 8, 1998 using the facility near-IR imager IRCAM3. IRCAM3 employs a  $256 \times 256$  InSb array; the optics used gives a pixel scale of  $0.280''$ . There was a small defocusing problem that occurred during these observations due to variable seeing, resulting in image elongation in the N-E, S-W direction. These uncertainties were estimated to be about  $1.2''$ . Continuum subtraction was not carried out because of the focusing problems in these images. It should also be noted that there is some ghosting that had occurred in these images. These are identified as ghost images since they occur at exactly the same position with respect to the main source both in object and standard star frames.

### 3. Results

The contour map of the spectrum shown in figure 1 displays the extended H<sub>2</sub> emission along the N-S direction (the slit axis) corresponding to the outflow axis. The intensity peaks at  $-3''$  and  $+2''$  represent H<sub>2</sub> knots in the outflow. From gaussian fits to the continuum emission pro-

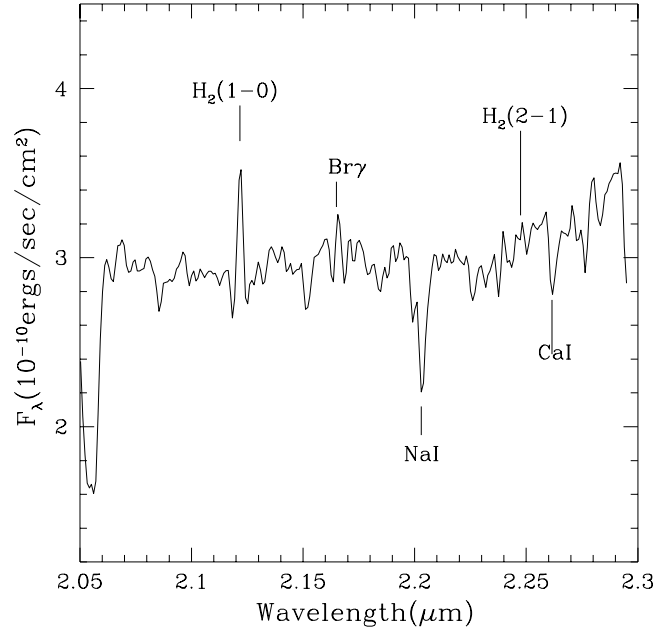


**Fig. 2.** Spectrum of RNO 91 integrated over 9 rows representing an area on-source of  $2'' \times 9''$ .

file at different positions along the dispersion axis, we find that the FWHM of the continuum strip (measured N-S) is about  $3.0''$ , although the seeing on the night of observation was between  $1.5$ - $2.0''$ . The extra width in the stellar continuum strip could be attributed to scattered light from the cocoon surrounding the star. We have therefore extracted the source spectrum by integrating the emission along three and then five rows, representing an on-source area of  $2'' \times 3''$  and  $2'' \times 5''$ . The relative intensities of the photospheric NaI and CaI features remained the same in these two extractions. However, in the  $3''$ -wide extraction, the  $2.122\mu\text{m}$  line intensity was considerably smaller relative to the photospheric features. This result confirms that the broadening of the continuum strip is indeed due to scattered star light.

Figure 2 shows the spectrum of RNO 91 in the wavelength region  $2.05\mu\text{m}$  to  $2.3\mu\text{m}$ . The spectrum is obtained by integrating nine rows, covering  $9''$  along the N-S slit axis centered around the star. The spectrum displays prominently the H<sub>2</sub>  $v=1-0$  S(1) line at  $2.122\mu\text{m}$  and the photospheric NaI and CaI absorption features at  $2.20\mu\text{m}$  and  $2.26\mu\text{m}$  respectively. The 2-1 S(1) line at  $2.247\mu\text{m}$  is below the noise level. The spectrum also displays the Br $\gamma$  emission line at  $2.167\mu\text{m}$ . These features are marked in the figure. Most of the other features seen in absorption are telluric in nature (Chelli et al. 1997).

The excitation mechanism for H<sub>2</sub> emission can be inferred from the 2-1 S(1)/1-0 S(1) flux ratio (e.g. Luhman et al. 1998). An estimated upper limit to the 2-1 S(1) line flux yields this ratio to be 0.16 or less, pointing strongly towards shock excitation. However, fluores-

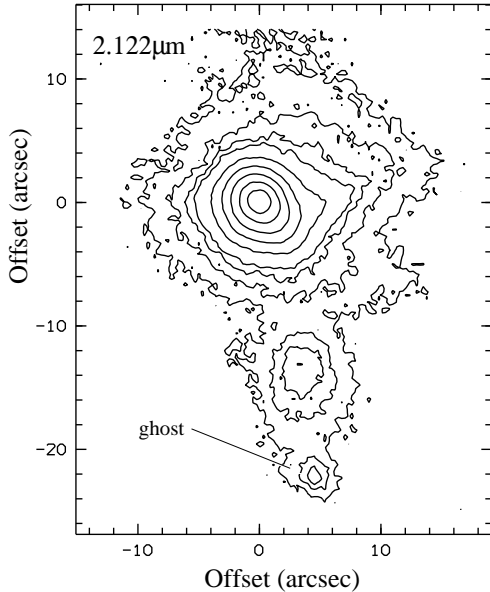


**Fig. 3.** Contour plot of RNO91 taken through narrowband filter, illustrating an east-west disk associated with the source, as well as nebulous emission to the south. The contours measure 5,10,15,20,40,80,160,320 and 640 $\times$  the standard deviation to the mean background level in the image.

cent excitation in a high density regime may also produce a “shock-like” 2-1 S(1)/1-0 S(1) ratio, because of thermalisation of low-energy vibrational levels (Sternberg & Dalgarno 1989, Burton et al. 1990). In a high density region one would still expect to see emission from the  $v=3$  level at 10% of the 1-0 S(1) line (rather than 1%, as is expected in a shock; see e.g. Luhman et al. 1998). However, in our spectrum the 3-2 S(3) line is unresolved from NaI absorption, and the 3-2 S(1) line is outside the wavelength range.

We resolve this issue by estimating the two most crucial parameters that decide the efficiency of the UV fluorescence, namely, the gas number density and the UV flux scaling parameter  $\chi$  (see Sternberg and Dalgarno 1989). We estimate an upper limit for the gas number density to be  $6 \times 10^5 \text{ cm}^{-3}$ , considering an  $A_v \sim 9$  (Myers et al. 1987), an outer disk radius of 1700AU (W94), and an inner disk radius of 0.01AU corresponding to the dust evaporating radius for an M0 star. Note that this density is for a gas disk of 1700AU and the actual regions from where we expect the H<sub>2</sub> emission are well below a radius of 200-300AU. On the other hand, the UV flux scaling parameter  $\chi$  for an M0 type star is much less than 1. From these, the UV fluorescence is expected to be of little significance for the excitation of H<sub>2</sub> lines.

Figure 3 shows a narrow band image through H<sub>2</sub> filter, without continuum subtraction. The disk structure and an

outflow lobe in the south can be seen clearly. These structures are more evident in this narrow band image, than in the earlier K' image of Hoddap (1994) or the polarimetric image of W94. W94 had shown the existence of frozen H<sub>2</sub>O, CO and possibly XCN in a disk structure of radius 1700AU around RNO 91. The existence of these ices on grains within this disk structure was proven by the absorption features found in a 3 – 5 $\mu\text{m}$  spectra. Their K-band polarimetric map also conforms with models of scattering from disks (Whitney & Hartmann 1992). W94 suggest a scenario with a flared disk viewed at an angle of 30 $^\circ$  with the northern outflow lobe tilted away from the observer. The narrow band image shown in figure 3 (note specifically the patch of continuum emission to the south of RNO 91) clearly support this scenario. In addition, it can be seen from fig 1 that the H<sub>2</sub> emission is extended more in the southern direction than in the northern direction which also confirms the tilt of the outflow axis, the northern lobe of the outflow being obscured near the source by the disk structure.

#### 4. Discussion

From the spectrum we measure an H<sub>2</sub> flux of  $7 \times 10^{-14} \text{ ergs sec}^{-2} \text{ cm}^{-2}$  (integrated over 3 rows, representing an area on-source of  $2'' \times 3''$ ). If we attribute this flux to shocks, we can estimate the mass flow rate  $\dot{M}$  using the relation

$$\epsilon L = G M \dot{M} / R = 1/2 \dot{M} v^2 \quad (1)$$

where  $\epsilon$  is the ratio of the total energy in the shock to the strength of the 1-0 S(1) line,  $L$  is the observed H<sub>2</sub> line luminosity, and  $v$  the shock velocity. We adopt a value for  $v$  of 30 km s<sup>-1</sup>, a value that is optimum for producing H<sub>2</sub> line emission. We also assume that  $\epsilon = 50$  (Smith 1995). Together, these yield an estimate for mass flux of  $\dot{M} = 4 \times 10^{-8} M_\odot \text{ yr}^{-1}$ .

As demonstrated in the previous section, the relative change in the intensity of H<sub>2</sub> from that of the photospheric features in the spectra extracted with different widths of the continuum strip shows that the H<sub>2</sub> emission close to the star likely originates from a region different to that traced by the photospheric lines. The fact that the H<sub>2</sub> line emission is extended along our N-S slit strongly suggests that the H<sub>2</sub> is associated with an outflow. By observing line emission coincident with the RNO 91 stellar continuum, we may therefore be tracing the outflow all the way back to the source. The total flux measured from the observed extended emission (integrated over 9 rows representing an area on-source of  $2'' \times 9''$ ) is  $1.5 \times 10^{-13} \text{ ergs sec}^{-2} \text{ cm}^{-2}$ . This represents an average flux distribution of  $3.5 \times 10^{-4} \text{ ergs sec}^{-2} \text{ cm}^{-2} \text{ sr}^{-2}$ . Assuming  $L_{H_2} \sim 10 \times L_{S(1)}$  (Davis & Eisloffel 1995), the extinction corrected S(1) line flux yields a net H<sub>2</sub> luminosity of  $0.002 L_\odot$ . Using the estimated value of  $\dot{M}$  and the kinematic age of the outflow, the H<sub>2</sub> luminosity can be shown to represent a net warm H<sub>2</sub> mass of  $\sim 5 \times 10^{-4} M_\odot$ , where,

a 9'' long flow with a velocity of 30 km s<sup>-1</sup> is used to calculate the age of the outflow.

The H<sub>2</sub> line flux measured from within the central 3'' could be associated with the near-IR counterparts of HH knots embedded within the cocoon that are excited by the outflow and accretion shocks in a disk. However, excitation of all of the observed “on-source” H<sub>2</sub> emission due to infall is not feasible, since the mass accretion rates derived from such infall will produce a K-band extinction (Herbst et al. 1995) that is an order of magnitude higher than the measured value by Myers et al. (1987). But some fraction of the observed emission could originate from accretion shocks, with the rest from the outflow, as in the case of T Tauri. It is interesting to note that the high resolution images obtained via Shift and Add imaging at UKIRT by A97 reveal a nebulous feature which is about 1'' north of the star. This could be a shock excited feature in the outflow. Alternatively, this feature – in conjunction with the fainter features to the S-W of the star – appears to be part of an ellipse whose major axis is  $\sim 200$  AU as measured by us using the published images of A97. In fact these features may be visualized in terms of a disk tilted by 30° to the north. The absence of any feature to the south may be attributed to the obscuration of the disk by the outflow. These arguments support the W94 data and their model, as do our narrow band images shown in Figure 3.

While gas and dust disks are known to exist around PMS stars (Beckwith et al. 1990, Dutrey et al. 1994), there exists a small sample of objects with disk structures that contain *icy mantles* where ices are found on dust particles in the protostellar envelopes (see Chiar et al. 1998 and references therein). RNO 91 possesses by far the largest icy gas/dust disk structure (20'') and also shows shocked H<sub>2</sub> originating in an outflow and possibly an accretion disk. These features make RNO 91 unique and an interesting object for further studies in millimeter and infrared wavelengths.

## 5. Conclusions

An infrared spectrum of RNO 91 shows emission of shocked molecular hydrogen from an outflow in the N-S direction and from a spatially unresolved region close to RNO 91. We estimate a mass flow rate of  $\dot{M} = 4 \times 10^{-8} M_{\odot} \text{ yr}^{-1}$ , based on the line fluxes from this spatially unresolved region around RNO 91. The line fluxes from the spatially extended outflow yield  $L_{H_2} \sim 0.002 L_{\odot}$  representing net warm H<sub>2</sub> mass of  $\sim 5 \times 10^{-4} M_{\odot}$ . The outflow seen here in H<sub>2</sub> emission, extending roughly N-S, appears to support the tilted disk + outflow model of W94, where the northern flow lobe is tilted away from us at an angle of 30° to the plane of the sky. Our narrow band images also support this scenario. We suggest that the H<sub>2</sub> flux from the spatially unresolved region around the source could originate in “HH-type” knots embedded in the co-

coon surrounding the star. However, accretion shocks cannot entirely be ruled out based on our observations. We argue that RNO 91 is a unique disk/outflow system.

*Acknowledgements.* This work is supported by the Department of Space, Government of India. The United Kingdom Infrared Telescope is operated by the Joint Astronomy Centre on behalf of the U.K. Particle Physics and Astronomy Research Council. The Imaging data reported here were obtained as part of the UKIRT Service Programme (obtained for us by Antonio Chrysostomou).

## References

- Aspin, C., Puxley, P. J., Hawarden, T. G., Paterson, M. J., & Pickup, D. A., 1997, MNRAS, 284, 257 (A97)
- Beckwith, S. V. W., Gatley, I., Matthews, K., & Neugebauer, G., 1978, ApJ, 223, L41
- Beckwith, S. V. W., Sargent, A. I., Chini, R. S., & Gusten, R., 1990, 99, 924
- Bence, S. J., Padman, R., Isaak, K. G., Wiedner, M. C., & Wright, G. S., 1998, MNRAS, 299, 965
- Burton M.G., 1992, Aust. J. Phys., 45, 463
- Burton M.G., Hollenbach D.J., Tielens A.G.G.M., 1990, ApJ, 365, 620
- Chelli, A., Cruz-Gonzalez, I., Salas, L., Ruiz, E., Carrasco, L., & Recillas, E., 1997, in eds. Malbet, F., & Castets, A., Low Mass Star Formation - From Infall to Outflow, poster proceedings of IAU Symp. No. 182.
- Chiar, J. E., Gerakines, P. A., Whittet, D. C. B., Pendleton, Y. J., Tielens, A. G. G. M., Adamson, A. J., & Boogert, A. C. A., 1998, ApJ, 498, 716
- Davis, C. J., & Eisloffel, J., 1995, A & A, 300, 851
- Dyck, H. M., Simon, T., & Zuckerman, B., 1982, ApJ, 255, L103
- Dutrey, A., Guilloteau, S., & Simon, M. 1994, A & A, 286, 149
- Herbst, T. M., Koresko, C. D., Leinert, C. 1995, ApJ, 444, L93
- Herbst, T. M., Beckwith, S. V. W., Glindemann, A., Tacconi-Garman, L. E., Kroker, H., & Krabbe, A. 1996, AJ, 111, 2403
- Heyer, M. H., Ladd, E. F., Myers, P. C., & Campbell, B., 1990, AJ, 99, 1585
- Hodapp, K. W., 1994, ApJSS, 94, 615
- Hora J.L., Latter, W.B., 1994, ApJ, 437, 281
- Koresko, C. D., Herbst, T. M., & Leinert, Ch., 1997, ApJ, 480, 741
- Leverault, R. M., 1988, ApJ, 330, 897
- Luhman K.L., Engelbracht C.W., Luhman, M.L., 1998, ApJ, 499, 799
- Myers, P. C., Fuller, G. A., Mathieu, R. D., Beichman, C. A., Benson, P. J., Schild, R. E., & Emerson, J. P., 1987, ApJ, 319, 340
- Myers, P. C., Heyer, M., Snell, R. L., & Goldsmith, P. F 1988, ApJ, 324, 907
- Schild, R., Nicholas, W., & Mathieu, R. D., 1989, AJ, 97, 1110
- Shull, J. M., & Beckwith, S., 1982, ARA&A, 20, 163
- Smith, M. D. 1995, A & A, 296, 789
- Sternberg, A., Dalgarno A., 1989, ApJ, 338, 197
- Weintraub, D. A., Tegler, S. C., Kastner, J. H., & Rettig, T., 1994, ApJ, 423, 674 (W94)
- Whitney, B. & Hartmann, L. 1992, ApJ, 395, 529